PRELIMINARY RESULTS FROM THE MOUNT WILSON SOLAR PHOTOGRAPHIC ARCHIVE DIGITIZATION PROJECT

L. BERTELLO, R.K. ULRICH, J.E. BOYDEN, and J. JAVARAIAH

UNIVERSITY OF CALIFORNIA, LOS ANGELES

SUMMARY

The Mount Wilson solar photographic archive digitization project makes available to the scientific community in digital form a selection of the solar images in the archives of the Carnegie Observatories (www.astro.ucla.edu/∼ulrich/MW_SPADP). This archive contains over 150,000 images of the Sun which were acquired over a time span in excess of 100 years. The images include broad-band images called White Light Directs, ionized CaK line spectroheliograms and Hydrogen Balmer alpha spectroheliograms. This project will digitize essentially all of the CaK and broad-band direct images out of the archive with 12 bits of significant precision and up to 3000 by 3000 spatial pixels. Solar images have been extracted and identified with original logbook parameters of observation time and scan format. The analysis of this data set will permit a variety of retrospective analyses of the state of the solar magnetism and provide a temporal baseline of about 100 years for many solar properties. The chromospheric network is clearly visible on a substantial fraction of the archive images from the CaK spectroheliogram sequence. The rate of solar rotation over the whole solar surface can be determined as a function of time using the day-to day motions of features on these CaK images. We present here preliminary results for the period 1915 to 1975. The pattern rotation rate is determined by cross-correlating observations taken on successive days for 11 separate latitude zones spanning the solar disk between ± 50 degrees in latitude.

CALIBRATION

The procedures used to calibrate the CaK images are described in some details at the project web site www.astro.ucla.edu/∼ulrich/MW_SPADP. We only provide here a short list of the most important steps included in this calibration process.

1. *Dust and pit removal*: these images present notably some dust and pit which is important to reduce. A Laplacian filter is used for this purpose.

2. *Image geometry*: radii and center of the image are determined using a quite complex iterative procedure which takes into account the distortion of the image. For this work an average value of the radius has been used.

3. *Center-to-limb variation*: one of the main problem we encountered during the calibration process is the presence of a vignetting function. This function is linked to the relative position between the pupil and the grating. As a result of this effect the intensity and its gradient are highly variable from one image to another. We currently remove this effect by using a running median filter to determine the background of the image and then divide the image by this background to obtain a flat image.

4. *Roll angle determination*: This information is available only for a limited number of images so that in general the roll angle needs to be determined directly from the image. Beginning 1935, polar marks indicating the solar north-south direction are present on most images and the roll angle can be easily calculated. However, a portion of the dataset includes images without any mark. A cross-correlation method is used in this case to determine the roll angle.

ANALYSIS

1. Each disk-oriented image is interpolated into a new 721×721 grid of equal longitude-interval and latitude-interval.

2. Only the central region between ± 60 degrees in longitude and ± 50 degrees in latitude is used.

3. 11 separate latitude zones are defined.

4. For each zone the rotation rate is calculated from:

$$\omega(\phi) = [\Delta L(\phi)]_{max}/\Delta t$$

where $[\Delta L(\phi)]_{max}$ is the value of the longitude lag with the maximum correlation, Δt is the difference in time between the two images, and ϕ is the latitude.

5. We determine the solar differential profiles by fitting the calculated $\omega(\phi)$ to least squares with the functional form:

$$\omega(\phi) = A + B\sin^2(\phi) + C\sin^4(\phi) \tag{1}$$

6. To remove the partial linear dependence between the terms for B and C we use the orthogonalized coefficients defined as:

$$\bar{A} = A + \frac{1}{5}B + \frac{3}{35}C; \qquad \bar{B} = \frac{1}{5}B + \frac{2}{15}C; \qquad \bar{C} = \frac{2}{21}C \tag{2}$$

CONCLUSIONS

- Because of the currently better determination of the roll angle for observations taken during the period 1935-1960, the number of calculated rotation rate values is much higher for that period than others (see the error bars in Figure 1).

- There is no indication of any significant periodicity in the temporal behavior of the orthogonalized rotation rate coefficients over the 60 years investigated in this work (see Figure 2).

- The difference between the orthogonalized coefficients calculated from the northern and southern hemispheres separately (Figure 3), for the period 1935-1960, shows that the A and B coefficients were higher (by $\sim$ 0.01 μrad/s) in the northern hemisphere than they were in the southern hemisphere.

- The average rotation rate of the Sun during the 20th century was higher during periods of minimum activity than it was during periods of maximum activity. The difference in the rotation rate at the equator can be estimated at about 0.01 microrad/s (see Figure 4).

- Future improvements in the current determination of the roll angle for images before 1935 and after 1960 are expected to produce more consistent results over the entire period investigated by this project.

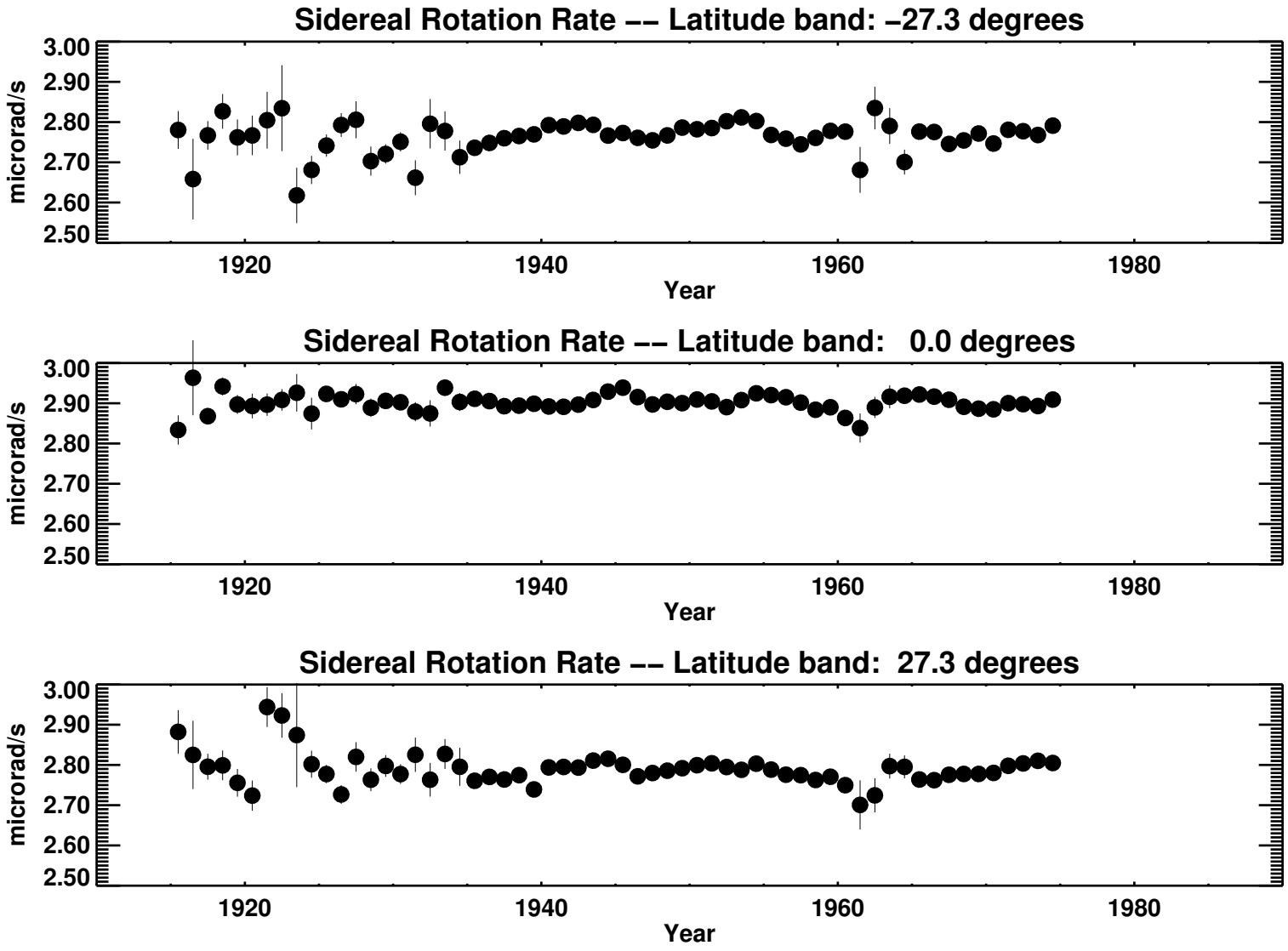

Figure 1. *Time dependence of solar surface rotation rate for 3 of the 11 latitude zones investigated in this work. Each point is the annual average of the calculated rotation rate values as described in the text. The error bars are 1-σ errors of the mean derived from the distribution of these values.*

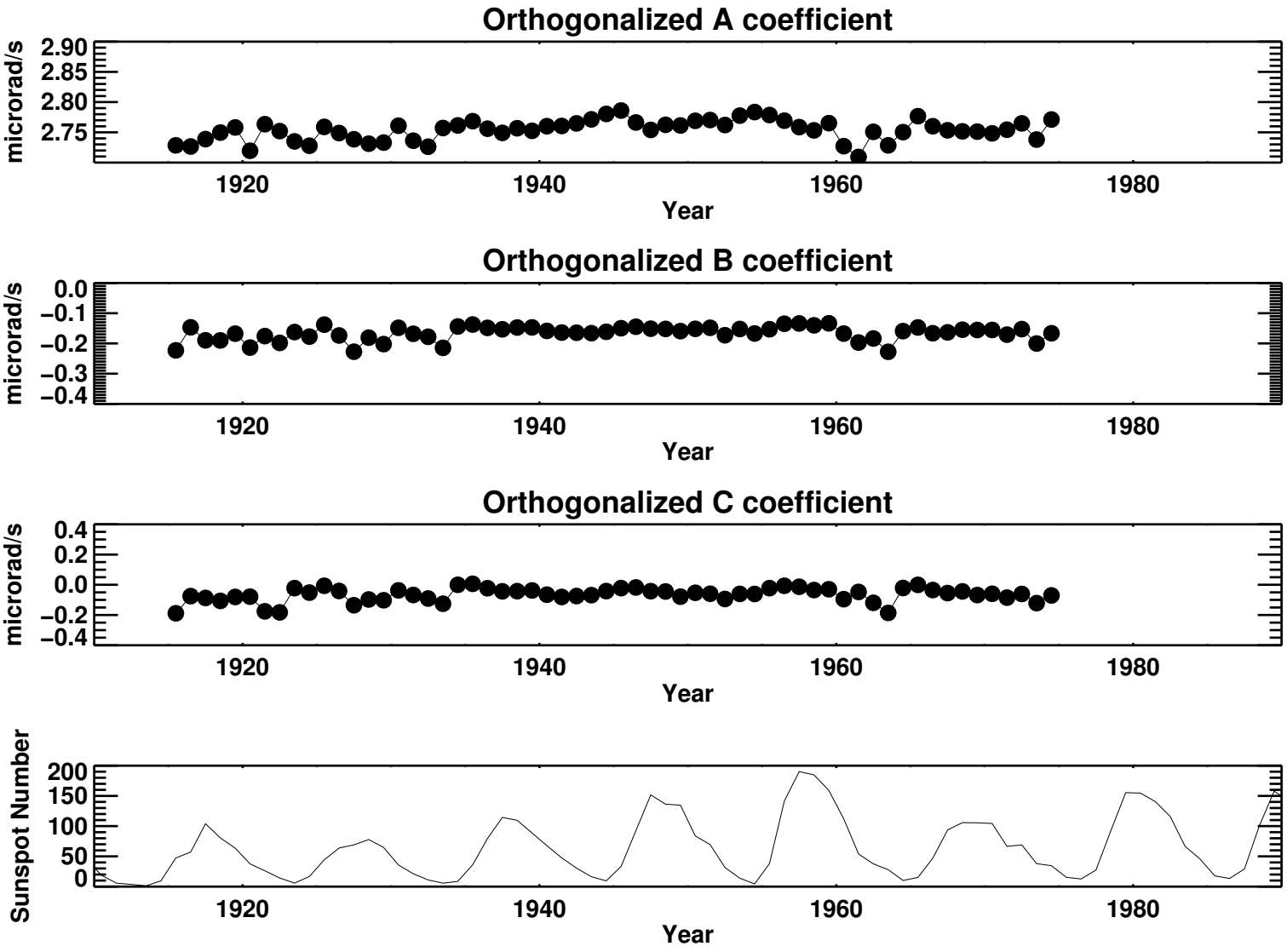

Figure 2. *Time dependence of the three orthogonalized rotation rate coefficients calculated according to Equations (1) and (2). The lower panel shows the annual averages of the international Sunspot Number obtained from the public NOAA databases at Boulder, Colorado.*

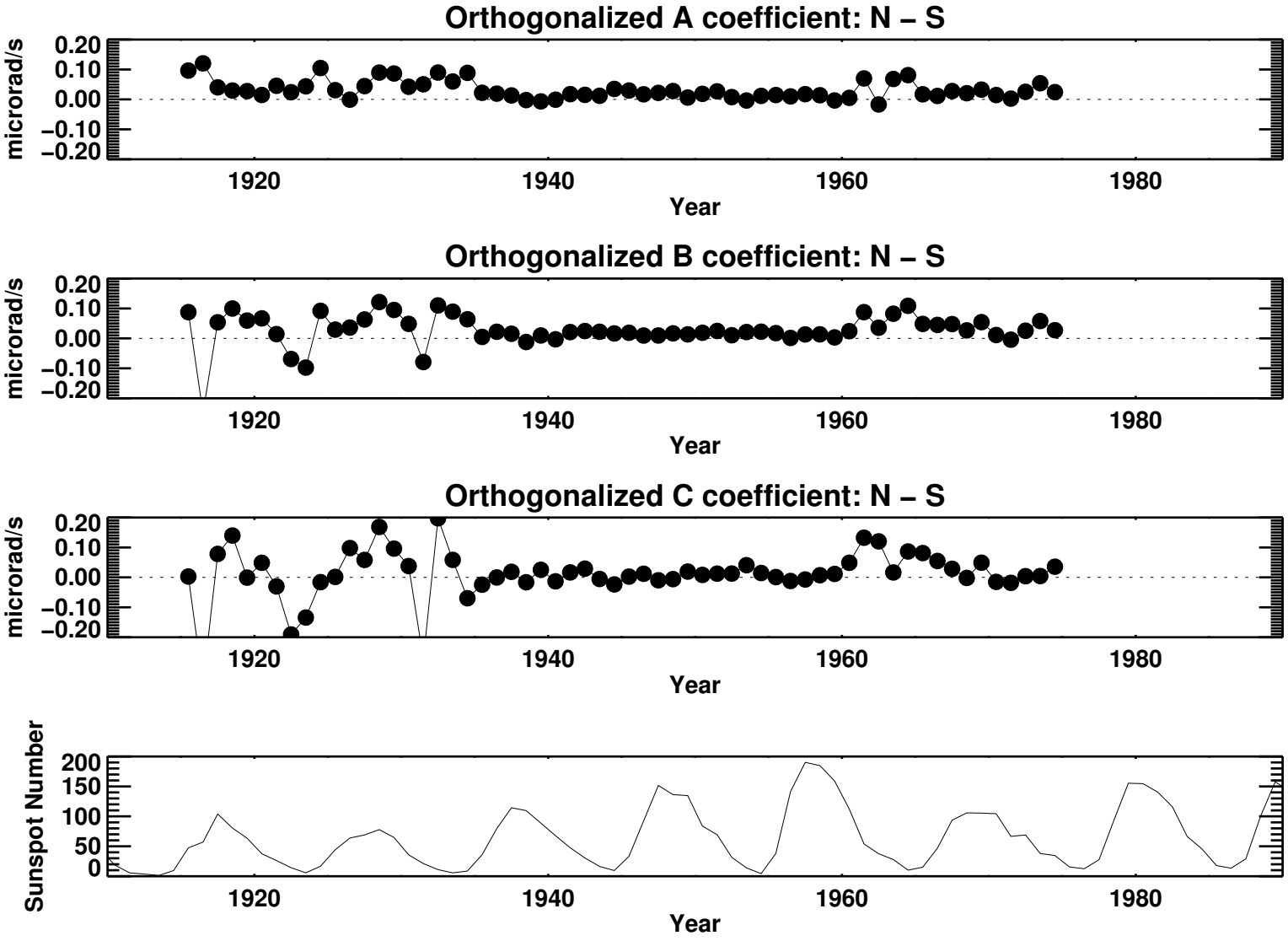

Figure 3. *Time dependence of the difference between the orthogonalized rotation rate coefficients calculated according to Equations (1) and (2) but using data from the northern and the southern hemispheres separately.*

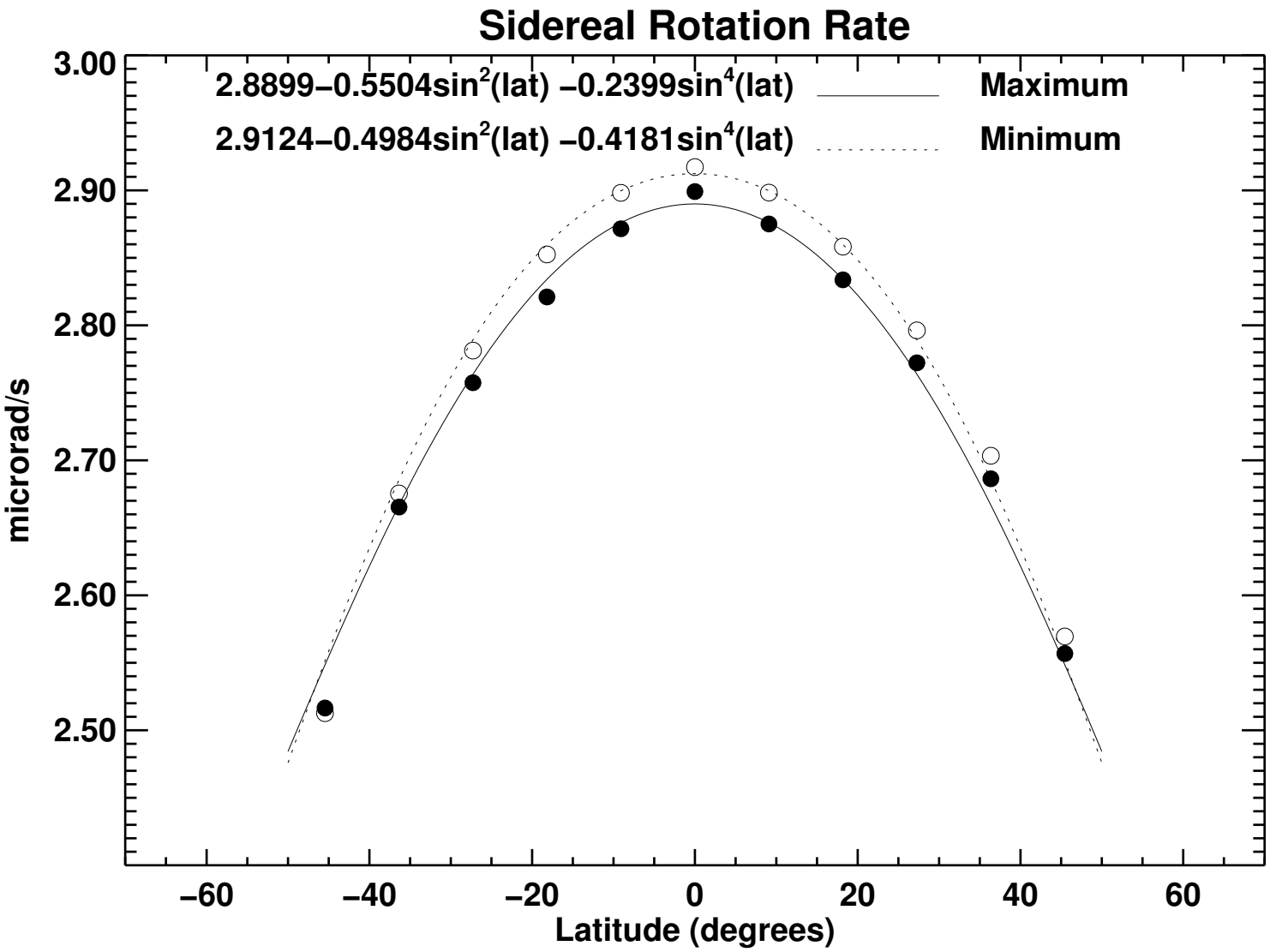

Figure 4. *Comparison between the average rotation rates determined during periods of maximum solar activity (filled circles) and periods of minimum (open circles) solar activity. All data from 1915 to 1975 were used to produce this plot. The error bars of each measurement are much smaller than the size of the points shown in the figure.*